

# Polymer Chemistry

Accepted Manuscript



This is an *Accepted Manuscript*, which has been through the Royal Society of Chemistry peer review process and has been accepted for publication.

*Accepted Manuscripts* are published online shortly after acceptance, before technical editing, formatting and proof reading. Using this free service, authors can make their results available to the community, in citable form, before we publish the edited article. We will replace this *Accepted Manuscript* with the edited and formatted *Advance Article* as soon as it is available.

You can find more information about *Accepted Manuscripts* in the [Information for Authors](#).

Please note that technical editing may introduce minor changes to the text and/or graphics, which may alter content. The journal's standard [Terms & Conditions](#) and the [Ethical guidelines](#) still apply. In no event shall the Royal Society of Chemistry be held responsible for any errors or omissions in this *Accepted Manuscript* or any consequences arising from the use of any information it contains.



Journal Name

ARTICLE

## Polymeric Palladium-Mediated Carbene Polymerization

Feifei Li, Longqiang Xiao and Lijian Liu\*

Received 00th January 20xx,  
Accepted 00th January 20xx

DOI: 10.1039/x0xx00000x

www.rsc.org/

Metalloenzyme-inspired polymeric palladium catalyst, which was prepared by self-assembly of polymeric imidazole ligand with PdCl<sub>2</sub>, promoted carbene polymerization with high catalytic activity and reusability. Besides the atactic polycarbethoxycarbene (PCEC), small amount of stereoregular PCEC was also obtained with poly(imidazole-Pd)-mediated polymerization of ethyl diazoacetate (EDA). This is the first example that stereoregular polycarbene in isolated form is obtained with a palladium-initiating system, suggesting that the steric polymeric imidazole ligand could affect the carbene insertion process. Detailed end group analyses on the obtained atactic and stereoregular PCEC revealed the chain initiation and chain termination mechanisms. XPS analyses on the oxidation state changes of palladium center exhibited that Pd<sup>II</sup> was reduced to Pd<sup>I</sup>, which suggests an intramolecular electron transfer process occurred during the interaction of palladium and EDA. Kinetic study showed a zero order kinetic dependent on the concentration of EDA, which indicates a strong binding of EDA on the catalyst preceding carbene formation. With the addition of radical inhibitor, the reaction rate was found to be greatly decreased. In the presence of spin trap, a striking electron paramagnetic resonance (EPR) spectrum could be detected, which suggests the involvement of radical intermediates. DFT calculations on the proposed Pd-carbene radical species supported the EPR analyses, which assigned a significant amount of spin density on the carbene-carbon atom. Based on these results, we proposed an unprecedented metal-carbene radical polymerization mechanism, which occurs through a stepwise carbene radical migration and insertion process to afford polycarbene.

### Introduction

Transition metal-mediated carbene polymerization is an attractive and efficient route to prepare densely functionalized polycarbene which are high-value polymer materials.<sup>1,2</sup> Palladium compounds are among the most active transition metal catalysts for carbene polymerization because of their high catalytic efficiency. Various Pd-based catalysts such as PdCl<sub>2</sub>, [PdCl<sub>2</sub>(MeCN)<sub>2</sub>], and [(N-heterocyclic carbene)Pd] are used as the catalytic precursors to induce polymerization of diazoacetates, diazoketones, and diazoacetamides, which typically produce atactic low molecular-weight polycarbene with high yields.<sup>3-5</sup> In the presence of tetraarylborate, [(N-heterocyclic carbene)Pd] was reported to produce higher molecular-weight polycarbene (*M<sub>n</sub>* up to 20000) with a certain extent control over the polymer tacticity,<sup>5</sup> which indicates that ligand variation could affect the catalytic reactivity of palladium catalyst, thus showing possibilities for obtaining stereoregular polycarbene with Pd-based catalysts by ligand design.<sup>6</sup> However, so far, except for the Rh<sup>I</sup>(diene) complexes and the [(N-benzyl-L-proline)Ir<sup>I</sup>(1,5-cyclooctadiene)] catalyst,<sup>7,8</sup> no sophisticated polycarbene

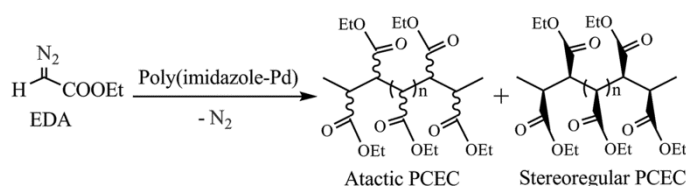
with high stereoregularity in isolated forms have been obtained with the reported Pd-based catalysts.<sup>9</sup>

Mechanistically, coordination of diazocompounds on the palladium centre and migratory insertion of carbene fragment into the growing polymer chain was generally proposed for palladium-mediated carbene polymerization. But competing suggestions about the oxidation states of palladium during the catalytic process still exist. While Ihara and coworkers proposed the *in situ* generated Pd<sup>II</sup>-alkyl species as the active species,<sup>3</sup> de Bruin and coworkers supposed the involvement of low-valent Pd species (Pd<sup>0</sup> or Pd<sup>I</sup>).<sup>9</sup> Even though the NMR spectra of the atactic polycarbene suggests a radical polymerization mechanism, the involvement of free radical species was excluded.<sup>9</sup> Thus, the exact nature of the active intermediate is still unclear and so far, the mechanisms of the chain initiation and termination processes have been poorly understood, which require more investigations.

Metalloenzyme-inspired polymeric metal catalysts, which catalyze high active and selective organic transformations with high efficiency, stability and reusability for sustainable and green chemistry, have attracted growing interest of the chemist community.<sup>10,11</sup> The polymeric imidazole-metal catalyst draws inspiration from galactose oxidase, which holds imidazole units in histidine coordinate to metal species to form the catalytic sites, the steric supramolecular structures could help to enhance catalytic selectivity.<sup>12-14</sup>

Department of Polymer Science, College of Chemistry and Molecular Sciences, Wuhan University, Wuhan 430072, China  
E-mail: liulj@whu.edu.cn

\*Electronic Supplementary Information (ESI) available: Fig. S1 to Fig. S8, Table S1 to Table S4. See DOI: 10.1039/x0xx00000x



**Scheme 1** Poly(imidazole-Pd)-mediated polymerization of EDA to produce atactic and stereoregular PCEC.

On our ongoing efforts in developing new catalysts and methods for carbene polymerization,<sup>15-17</sup> we report that the polymeric imidazole-palladium complexes (poly(imidazole-Pd)), which was prepared by self-assembly of PdCl<sub>2</sub> and poly[(*N*-vinylimidazole)-*co*-(*N*-isopropylacrylamide)], could offer high catalytic activity and reusability for polymerization of ethyl diazoacetate (EDA) as well as produce a small amount of stereoregular polycarbomethoxycarbene (PCEC) (Scheme 1). Since the heterogeneous poly(imidazole-Pd) catalyst could be easily separated from the reaction mixture, the oxidation state change of palladium centre could be feasibly probed by X-ray photoelectron spectroscopy (XPS). With the help of online infrared (IR) spectroscopy, the effect of the radical inhibitor 2, 2, 6, 6-tetramethylpiperidine-1-oxyl (TEMPO) on the polymerization process could be traced *in situ*, thus we re-investigated the possibility of palladium-initiated carbene radical polymerization process. Electron paramagnetic resonance (EPR) spectroscopy, which could provide direct evidence for detecting paramagnetic species, was also used to characterize the poly(imidazole-Pd)-catalyzed carbene polymerization reaction. In the presence of spin trap *N*-tert-butyl- $\alpha$ -phenylnitron (PBN), the appearance of the striking EPR signal provides unequivocal spectroscopic evidence for the existence of the radical intermediates.<sup>18</sup> DFT calculations on the proposed Pd-carbene radical species supported the EPR analyses, which assigned large amount of spin density on the carbene moiety. Based on these results, we further proposed an unprecedented metal-carbene radical polymerization (MCRP) mechanism, which occurs through a stepwise carbene radical migration and insertion process to produce polycarbomethoxycarbene. The MCRP strategy amalgamates traditional coordination polymerization mechanism with radical polymerization mechanism, but distinguishes from either of the two.

## Experimental Section

### Methods

All experiments were carried out in distilled solvents under N<sub>2</sub> atmosphere. 2,2,6,6-tetramethylpiperidine 1-oxyl (TEMPO, 98%, Aldrich) and *N*-tert-Butyl- $\alpha$ -phenylnitron (PBN, 98%, Aldrich) were stored at -20 °C and used as received. EDA was prepared with glycine ethyl ester hydrochloride and sodium nitrite in cold ethyl ether. The obtained ether solution of EDA were subjected to distillation at 20 °C until ether was removed and pure EDA was obtained as yellow residual oil.<sup>19</sup>

<sup>1</sup>H and <sup>13</sup>C NMR spectra were recorded on a Mercury VX-300 spectrometer (300 MHz) using CDCl<sub>3</sub> as solvent and trimethylsilane (TMS) as the internal standard. The number-average molecular weight (*M<sub>n</sub>*) and polydispersity index (PDI, *M<sub>w</sub>/M<sub>n</sub>*) of the polymer samples were determined by gel permeation chromatography (GPC) calibrated with polystyrene standards in THF solution (1.0 mL min<sup>-1</sup>) at 30 °C and GPC is equipped with a Waters 717 plus auto sampler, a Waters 1515 isocratic HPLC pump, a Waters 2414 refractive index detector, and Shodex K-805, K-804, and K-802.5 columns in series. Matrix-assisted laser desorption/ionization time of flight (MALDI-TOF) mass spectrometric analyses were performed on Shimadzu Biotech Axima TOF spectrometer. Online infrared (IR) spectra were collected on an is10 (Thermo) with a fiber optical system (MultiLoop-MIR) designed for infrared sampling of liquids (detection range: 1600-3400 cm<sup>-1</sup>). Scanning electron microscopy (SEM) observation was done by a Sirion 200 field emission scanning electron microscope (FEI Co., Eindhoven). Energy dispersive X-ray spectroscopy (EDX) spectrum was recorded by JEM-2100 (HR) using nickel screen as sample carriers. Wide-angle X-ray diffraction (WAXD) measurements were performed on Shimadzu XRD-6000 X-ray diffractometer with a Ni-filtered Cu K $\alpha$  radiation source ( $\lambda=0.154$  nm, 40 KV, 30 mA). X-ray photoelectron spectroscopic (XPS) measurements were performed on an X-ray photoelectron spectroscopy (XSAM800, Kratos, UK).

### Preparation of poly(imidazole-Pd) catalyst

The poly(imidazole-Pd) was prepared by self-assembly of PdCl<sub>2</sub> and poly[(*N*-vinylimidazole)-*co*-(*N*-isopropylacrylamide)] in CHCl<sub>3</sub>/H<sub>2</sub>O at 70 °C in the presence of CH<sub>3</sub>OH *via* coordinative convolution method.<sup>12-14</sup> The obtained poly(imidazole-Pd) catalyst was washed with large amount of water and CHCl<sub>3</sub> and vacuum dried before use.

### Poly(imidazole-Pd)-mediated polymerization of EDA

A solution of toluene (10 ml) and poly(imidazole-Pd) catalysts (50 mg) was stirred under N<sub>2</sub> at predetermined temperature for 30 min and then EDA (1 ml, 9.45 mmol) was introduced to the system. After 17 hours of reaction, the heterogeneous catalysts were isolated and the filtrates were concentrated to precipitate from petroleum ether. The obtained viscous products were re-dissolved in CHCl<sub>3</sub> to allow for two more precipitation from Et<sub>2</sub>O, from which small amount of solid products were obtained.

### Kinetic studies of poly(imidazole-Pd)-mediated polymerization of EDA using online IR spectroscopy

A solution of toluene (10 ml), poly(imidazole-Pd) catalysts (30 mg) was stirred under N<sub>2</sub> for 10 min at pre-determined temperature and then EDA (300 mg, 2.63 mmol) was introduced to the system to start the polymerization reaction as well as the data collection. The disappearance of the 2110 cm<sup>-1</sup> stretching band was followed continuously to depict the decomposition dynamics of EDA in the presence of poly(imidazole-Pd). Kinetic traces were simulated by fitting to a sum of exponential equations.

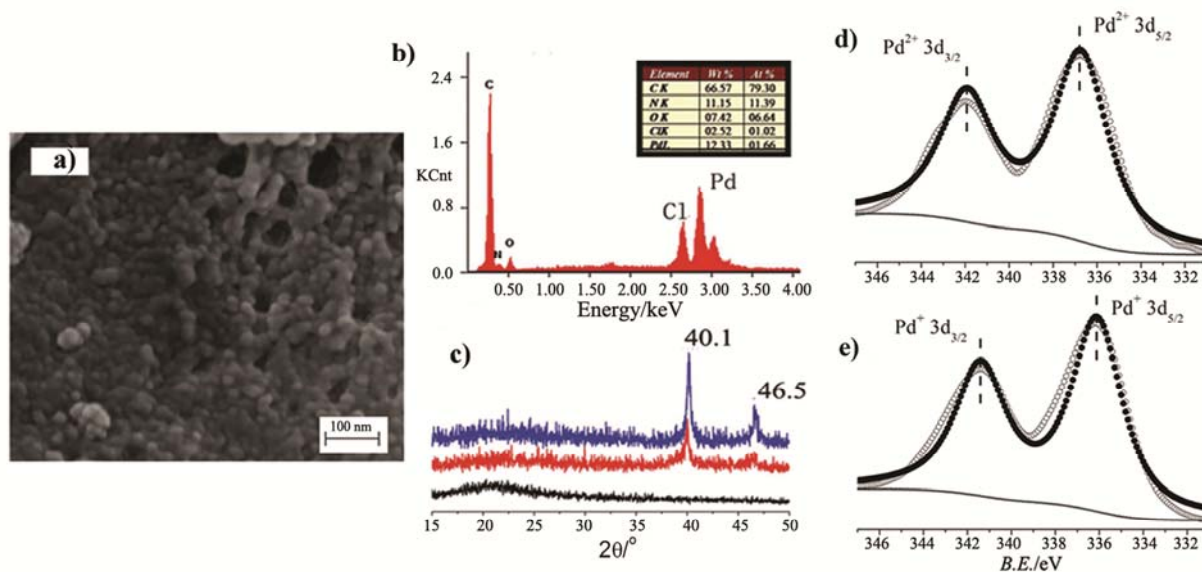


**Fig. 1** Characterization of poly(imidazole-Pd): SEM image (a); EDX/SEM image (b); XRD diffraction spectra (before reaction (blue line), after reaction (red line), and pure poly[(*N*-vinylimidazole)-*co*-(*N*-isopropylacrylamide)] (dark line) (c); XPS spectra with fit before use (d) and after use (e).

### Radical inhibition experiment

A solution of toluene (10 ml), TEMPO (0.1 g, 0.64 mmol) and poly(imidazole-Pd) (50 mg) was stirred under  $N_2$  at  $60^\circ C$  for 5 min and then EDA (500  $\mu L$ , 4.73 mmol) was introduced to the system. The disappearance of the  $2110\text{ cm}^{-1}$  stretching band was followed continuously to depict the decomposition dynamics of EDA in the presence of TEMPO.

### Spin-trapping experiment

A solution of toluene (5 ml), PBN (30 mg, 0.17 mmol) and metal catalysts (30 mg) were stirred under  $N_2$  at  $60^\circ C$  for 5 min, after strict extrusion of  $O_2$ , EDA (500  $\mu L$ , 4.73 mmol) was introduced to the systems. Then immediately 2  $\mu L$  of the solution was collected and detected by room-temperature EPR.

### EPR analyses

X-band EPR spectra were recorded on Bruker Biospin A200 spectrometer. The spectrum was simulated by iteration of the anisotropic *g*-values, hyperfine coupling constants, and line widths using Biomolecular EPR Spectroscopy Software developed by W. R. Hagen.

### DFT calculations

Geometry of Pd-carbene radical was optimized by BP86 density functional method in combination with def2-SVP basis-set. When evaluating single-point energies, the basis-set used was upgraded to def2-TZVP. ORCA 3.0.3 program was used to conduct the calculations. Multiwfn 3.3.7 program was employed to calculate spin density and spin population was obtained *via* Mulliken method.

## Results and discussion

The novel poly(imidazole-Pd) catalyst was prepared by self-assembly of  $PdCl_2$  and poly[(*N*-vinylimidazole)-*co*-(*N*-isopropylacrylamide)] in  $CHCl_3/H_2O$  solution at  $70^\circ C$  *via* coordinative convolution method<sup>12-14</sup> and its aggregation structure was characterized by SEM, EDX, XRD and XPS techniques (Fig. 1). The SEM image (Fig. 1a) reveals the mesoporous suprastructure of the catalyst with its surface covered with nanometers globular particles (10 to 20 nanometers in diameter), which could increase the catalytic area. The EDX/SEM image shows the existence of palladium species (the loading of palladium is about 12%, Fig. 1b). The peaks at  $2\theta = 40.1^\circ$  and  $46.5^\circ$  on the XRD spectrum (Fig. 1c) exhibits the crystalline palladium in poly(imidazole-Pd) and the broad peaks centred at  $2\theta$  around  $22^\circ$  exhibits the polymeric imidazole matrix.<sup>20</sup> XPS analysis (Fig. 1d) of Pd  $3d_{5/2}$  shows the binding energy value of 336.93 eV, which is assigned to Pd(II) species.<sup>21</sup> These results indicate that palladium coordinated on the polymeric imidazole ligands to form polymeric imidazole-palladium complex.

Carbene polymerization reactions were conducted with a catalytic amount of poly(imidazole-Pd) (2 mol% Pd) and ethyl diazoacetate (EDA) in toluene for 17 h. After the catalyst was isolated, the reaction mixture was decanted into petroleum ether, from which, large amount of crude products were obtained as viscous oil in 79~95% yields (Table 1). Further reprecipitated the viscous product from  $Et_2O$ , small amount of solid product could also be successfully isolated (~5% yields). The catalyst was reused at  $60^\circ C$  for five times without loss of catalytic activity (entries 6-10), suggesting that the newly

**Table 1** Poly(imidazole-Pd)-mediated polymerization of EDA<sup>a</sup>

run	temperature (°C)	yield (%) <sup>b</sup>	$M_n$ (g mol <sup>-1</sup> ) <sup>c</sup>	$M_w$ (g mol <sup>-1</sup> ) <sup>c</sup>	PDI $M_w/M_n$ <sup>c</sup>
1	30	79	1240	1600	1.28
2	40	89	1090	1310	1.20
3	60	79	1680	2510	1.49
4	70	80	910	1080	1.19
5	100	95	800	1020	1.50
6 (1st reuse)	60	84	1530	1910	1.24
7 (2nd reuse)	60	83	910	1200	1.32
8 (3rd reuse)	60	77	800	940	1.17
9 (4th reuse)	60	87	910	1100	1.20
10 (5th reuse)	60	95	910	1170	1.28

<sup>a</sup> Experimental conditions: 50 mg Poly(imidazole-Pd), 1 ml EDA, 10 ml toluene, 17 h. Crude products were obtained by precipitating from petroleum ether. <sup>b</sup> Yield% = [the weight of the products]/[the weight of monomer- $9.45 \times 10^{-3} \times 28$ ]\*100%. <sup>c</sup>  $M_n$ ,  $M_w$  and PDI ( $M_w/M_n$ ) were obtained by GPC calibration using standard polystyrenes in THF solution.

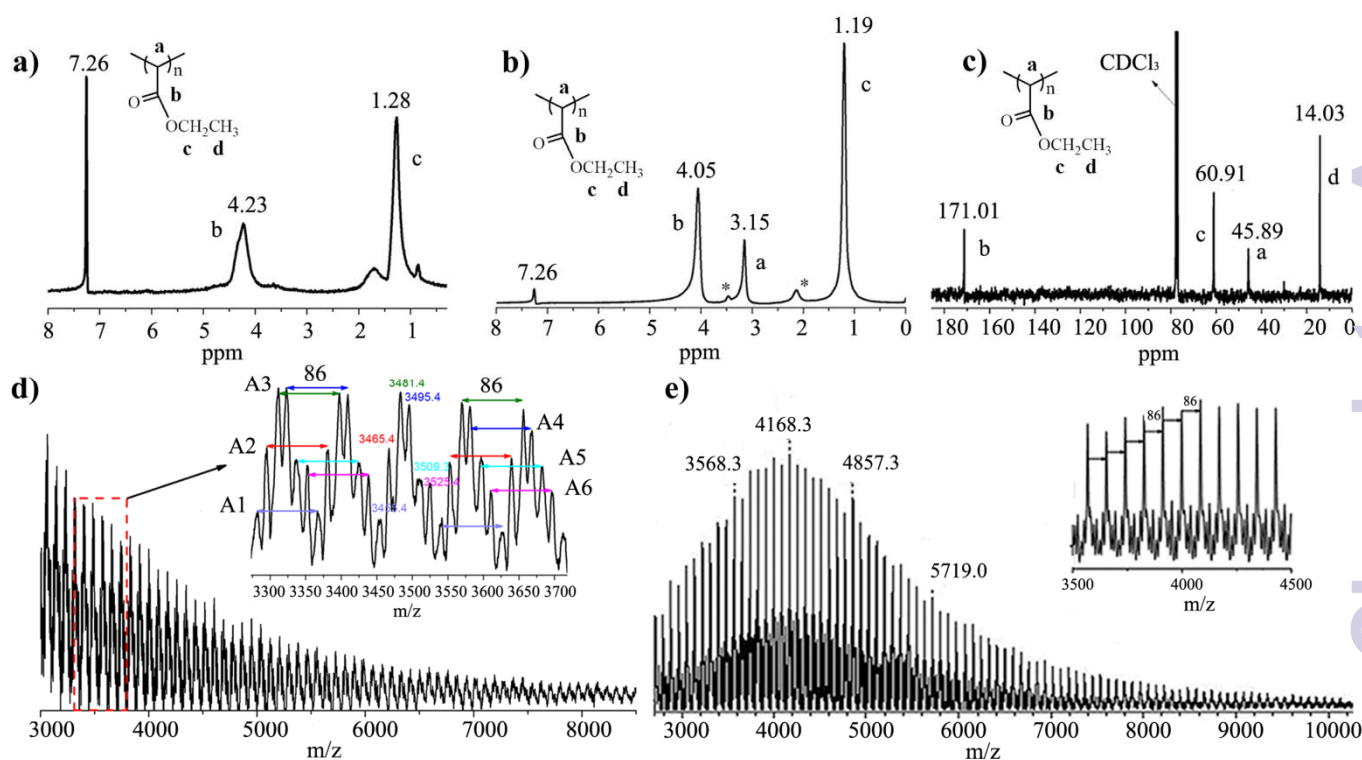


**Fig. 2** Characterization of atactic and stereoregular PCEC. (a) <sup>1</sup>H NMR spectrum of atactic PCEC; <sup>1</sup>H NMR spectrum of stereoregular PCEC (b; the additional peaks marked \* at 3.5 ppm and 2.1 ppm refer to the impurity ether and H<sub>2</sub>O respectively) and <sup>13</sup>C NMR spectrum of stereoregular PCEC (c); (d) MALDI-TOF mass spectrum with  $m/z$  from 3000 to 8500 for atactic PCEC. The inset of (d) is  $m/z$  from 3300 to 3700. The series are assigned to **A1**: H-[CH(COOEt)]<sub>n</sub>-CH<sub>3</sub>, (e.g.,  $m/z=3455.4$ ,  $n=40$ ); **A2**: Na<sup>+</sup>{H-[CH(COOEt)]<sub>n</sub>-H}, (e.g.,  $m/z=3465.4$ ,  $n=40$ ); **A3**: Na<sup>+</sup>{H-[CH(COOEt)]<sub>n</sub>-OH}, (e.g.,  $m/z=3481.4$ ,  $n=40$ ); **A4**: Na<sup>+</sup>{H-[CH(COOEt)]<sub>n</sub>-OCH<sub>3</sub>}, (e.g.,  $m/z=3495.4$ ,  $n=40$ ); **A5**: Na<sup>+</sup>{H-[CH(COOEt)]<sub>n</sub>-OCH<sub>2</sub>CH<sub>3</sub>}, (e.g.,  $m/z=3509.3$ ,  $n=40$ ); **A6**: {H-[CH(COOEt)]<sub>n</sub>-(COOEt)C=CH(COOEt)}, (e.g.,  $m/z=3525.4$ ,  $n=39$ ). (e) MALDI-TOF mass spectrum with  $m/z$  from 3000 to 10000 for stereoregular PCEC. The inset of (e) is  $m/z$  from 3500 to 4500. The main peaks correspond to Na<sup>+</sup>{H-[CH(COOEt)]<sub>n</sub>-OH}, (e.g.  $m/z=4857.3$ ,  $n=56$ ).

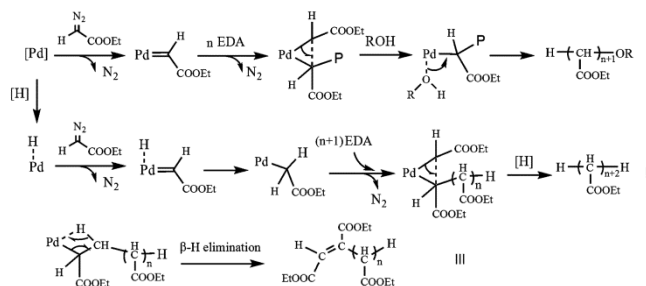
developed poly(imidazole-Pd) catalyst could provide high catalytic activity and reusability for carbene polymerization.

The  $^1\text{H}$  NMR spectrum of the viscous product (Fig. 2a) shows very broad resonance, which is indicative for atactic polycarbethoxycarbene (PCEC), while the  $^1\text{H}$  and  $^{13}\text{C}$  NMR spectra of the solid product exhibit surprisingly sharp resonance (Fig. 2b and 2c), indicative for stereoregular PCEC.<sup>7</sup> Clearly, the polymer main chain methine (-CH-) signal appears as highly symmetrical singlet at  $\delta=3.15$  ppm on  $^1\text{H}$  NMR spectrum (Fig. 2b) and 45.89 ppm on  $^{13}\text{C}$  NMR spectrum, and the carbonyl signal gives rise to  $^{13}\text{C}$  NMR shift at 171.01 ppm (Fig. 2c), which are similar to those of syndiotactic polymer obtained by the Rh(diene)-initiating systems (45.40 ppm for methine and 170.80 ppm for carbonyl).<sup>6</sup> The result reveals that besides atactic PCEC, highly stereoregular PCEC is also generated by the poly(imidazole-Pd)-mediated polymerization of EDA, which, as far as we know, is the first example that stereoregular polycarbene in isolated form is obtained with a palladium-initiating system.

Both the MALDI TOF mass spectra of the atactic PCEC (Fig. 2d) and the stereoregular PCEC (Fig. 2e) show peaks with repeating units of 86 Da [ $\text{CH}(\text{COOEt})$ ], confirming chain-propagation occurs through carbene insertion.<sup>22</sup> Remarkably, while the MALDI-TOF mass spectrum of the stereoregular PCEC reveals only one set of strong signals corresponding to  $(86n+41)$  Da, which is interpreted as:  $\text{Na}^+\{\text{H}-[\text{CH}(\text{COOEt})]_n-\text{OH}\}$  (e.g.,  $m/z=4857.3$ ,  $n=56$ ), the mass spectrum of the atactic PCEC reveals six main sets of signals corresponding to polymer chains  $\{\text{H}-[\text{CH}(\text{COOEt})]_n-\text{E}\}$  (E refers to different end groups; series A1 to A6 in the inset of Fig. 2d). The predominating  $\text{Na}^+\{\text{H}-[\text{CH}(\text{COOEt})]_n-\text{OH}\}$  (e.g.,  $m/z=3481.4$ ,  $n=40$ ; A3),  $\text{Na}^+\{\text{H}-[\text{CH}(\text{COOEt})]_n-\text{OCH}_3\}$  (e.g.,  $m/z=3495.4$ ,  $n=40$ ; A4), and  $\text{Na}^+\{\text{H}-[\text{CH}(\text{COOEt})]_n-\text{OCH}_2\text{CH}_3\}$  (e.g.,  $m/z=3509.3$ ,  $n=40$ ; A5) signals indicate the prevalence of the chain transfer-process induced by the trace amounts of  $\text{H}_2\text{O}$ ,  $\text{CH}_3\text{OH}$  and  $\text{CH}_3\text{CH}_2\text{OH}$  within the reaction systems (Scheme 2I).<sup>22</sup> The appearance of the  $\text{Na}^+\{\text{H}-[\text{CH}(\text{COOEt})]_n-\text{H}\}$  signal (e.g.,  $m/z=3465.4$ ,  $n=40$ ; A2) implies the generation of “palladium-hydrogen” species as an initiating species and chain-termination may occur by protonation of the growing oligomer chain (Scheme 2II). The little  $\{\text{H}-[\text{CH}(\text{COOEt})]_n-(\text{COOEt})\text{C}=\text{CH}(\text{COOEt})\}$  signal (e.g.,  $m/z=3525.4$ ,  $n=39$ ; A6) suggests a minor role of the  $\beta$ -H elimination-termination process (Scheme 2III).<sup>5,23</sup>

We further investigate the influence of alcohol and water on the obtained oligomer yield and molecular weight (Table S1<sup>†</sup>). With the addition of water, methanol and ethanol, lower oligomer yields and molecular weight ( $M_n$ ) were produced. These results indicated that water, methanol and ethanol could deactivate the catalyst at high amount while they could be chain-transfer agents at extremely low amount.<sup>22</sup>

Besides, the observation that the stereoregular PCEC show higher polymerization degree than atactic PCEC and they have different spectroscopic patterns point to the presence of different active species, differing in their chain-propagation behavior.<sup>9</sup> The increased steric hindrance of the poly(imidazole) ligands on the palladium centre could affect the carbene



**Scheme 2** Proposed chain-initiation, chain-transfer and chain-termination mechanisms for poly(imidazole-Pd)-mediated carbene polymerization.

insertion steps and improve the stereoselective chain propagation that leads to the generation of stereoregular PCEC

As a heterogeneous catalyst, poly(imidazole-Pd) could be isolated from the reaction mixture and the oxidation state changes of the metal catalyst could be directly characterized by XPS. As shown in Fig. 1e, the binding energy value of  $\text{Pd } 3d_{5/2}$  shifts from 336.93 eV ( $\text{Pd}^{2+}$ ) to 336.06 eV, which is higher than the normal binding energy value of  $\text{Pd}^0 3d_{5/2}$  (335.5 eV)<sup>24</sup> and is assigned to  $\text{Pd}^+$   $3d_{5/2}$ .<sup>9</sup> The result that  $\text{Pd}^{\text{II}}$  was reduced to  $\text{Pd}^{\text{I}}$  clearly suggests that an intra-molecular electron transfer process occurred during the interaction of palladium catalyst and EDA.<sup>25</sup>

To further explore the carbene polymerization mechanism, the process of poly(imidazole-Pd)-mediated polymerization of EDA was monitored by online IR spectroscopy.<sup>26</sup> Fig. 3a and 3b show the corresponding 3-D and 2-D IR spectra of the absorption bands between 2200  $\text{cm}^{-1}$  and 1600  $\text{cm}^{-1}$ . Besides the steady disappearance of EDA ( $\nu_{\text{CH}=\text{N}_2}$  at 2110  $\text{cm}^{-1}$  and  $\nu_{\text{C}=\text{O}}$  at 1705  $\text{cm}^{-1}$ ), the formation of another absorption band at 1740  $\text{cm}^{-1}$  (possibly due to the  $\text{C}=\text{O}$  stretching of oligomer) is also observed.<sup>27</sup> Tracing the steady disappearance of the absorption band at 2110  $\text{cm}^{-1}$ , a zero order kinetics dependent on EDA concentration is fit for the polymerization reaction (Fig. S1<sup>†</sup>). Fig. 3c shows that the relationship between the real time concentration of EDA and the reaction time, which is consistent with a linear fit curve. The deviation from the kinetic profile at the incipient stage is designated the existence of an induction period. The long reaction time indicates that only a small fraction of palladium is active in the catalytic process.

We further conduct kinetic studies by varying the amount of poly(imidazole-Pd) catalyst (Fig. S2<sup>†</sup>) and the concentration of EDA (Fig. S3<sup>†</sup>), the polymerization processes are consistent with zero-order rate law. The observation of zero order substrate dependency indicates that a strong pre-equilibrium binding of EDA on poly(imidazole-Pd) occurred preceding the carbene formation.<sup>28</sup>

The kinetic profiles of the five-time-reuse reactions were also recorded (Fig. S4<sup>†</sup>). It is interesting to note that while the reaction rates decreased with the reuse times, the highest oligomer yield (95%) was obtained with the fifth reuse experiment, in which the catalytic rate was the slowest.

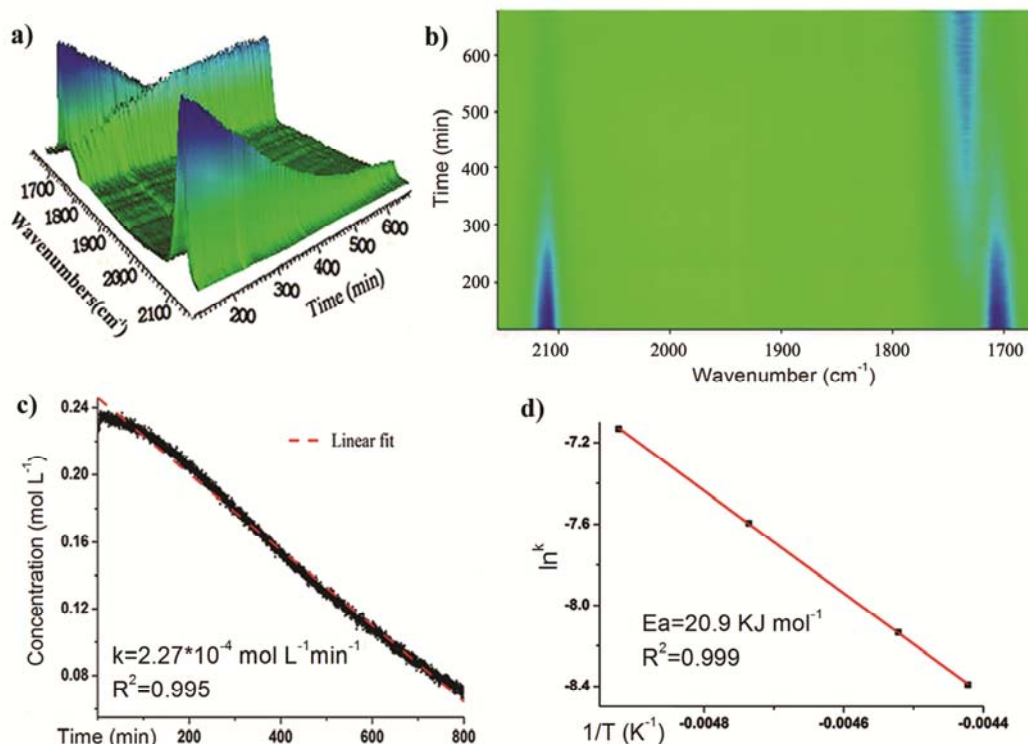


**Fig. 3** (a) 3-D and 2-D IR spectra of poly(imidazole-Pd)-mediated polymerization of EDA process; (c) zero order kinetics plot fits for the polymerization reaction (conditions: 30 mg poly(imidazole-Pd), 2.63 mmol EDA, 10 ml toluene, temperatures were set at 47, 52, 62, and 70 °C, Fig. S1†); (d) Arrhenius plot to calculate the apparent activation energy ( $E_a$ ) value (Table S2†).

The apparent activation energy ( $E_a$ ) was estimated to be 20.9 kJ/mol (Fig. 3d), which reveals the low reaction barrier and indicates a radical polymerization mechanism.<sup>16</sup> Since it is not possible to isolate the intermediates due to their high reactivity, the effect of the radical inhibitor 2, 2, 6, 6-tetramethylpiperidine-1-oxyl (TEMPO) on the polymerization process was investigated by online IR spectroscopy to probe the possibility of radical polymerization mechanism.<sup>9</sup>

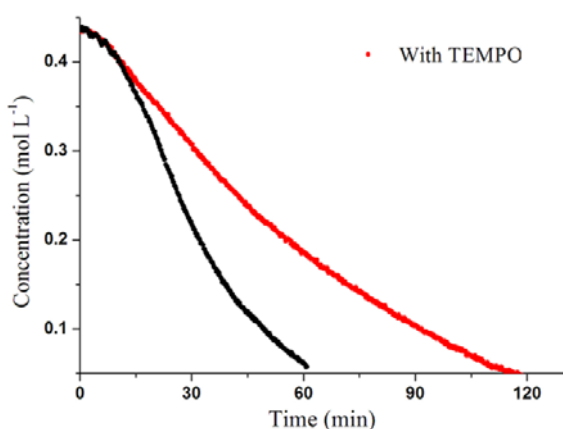


**Fig. 4** The effect of TEMPO on the process of poly(imidazole-Pd)-mediated polymerization of EDA (conditions: 50 mg poly(imidazole-Pd), 4.73 mmol EDA, 10 ml toluene, 0.64 mmol TEMPO, 60 °C).

Poly(imidazole-Pd)-mediated polymerization of EDA was then conducted with the addition of TEMPO (0.64 mmol), and the disappearance of the absorption band at 2110  $\text{cm}^{-1}$  was also tracked by online IR spectroscopy. As shown in Fig. 4, although the conversion of EDA could not be completely blocked, the reaction rate was obviously decreased as the reaction time with TEMPO prolonged to more than 120 min. While without TEMPO, the reaction finished in about 60 min. The effect of TEMPO on the oligomer yields and molecular weight was also analyzed (Table S3†). With the addition of TEMPO, the oligomer yields dramatically reduced while the molecular weight ( $M_n$ ) slightly decreased. Previously, an unique carbon-centred cobalt<sup>III</sup>-carbene radical<sup>29</sup> in the  $[\text{Co}^{\text{II}}(\text{Por})]$ -ethyl styryldiazoacetate system was reported to be intercepted by TEMPO,<sup>30</sup> so we supposed that similar carbon-centred Pd-carbene radical was also generated with the poly(imidazole-Pd)-EDA system.<sup>31</sup>

We resort to use *N-tert*-butyl- $\alpha$ -phenyl nitone (PBN) as spin trap to detect the radical intermediates.<sup>32</sup> PBN has been successfully used to identify carbon-centred radical intermediates in organocobalt-mediated radical polymerization reactions.<sup>18</sup> To our delight, monitoring poly(imidazole-Pd)-mediated polymerization of EDA in the presence of PBN led to a clear electron paramagnetic resonance (EPR) spectrum that is assigned to the adducts of PBN and radical intermediates (Fig. 5).<sup>33</sup> The EPR spectrum has been simulated to have hyperfine coupling constants (HFCs) of

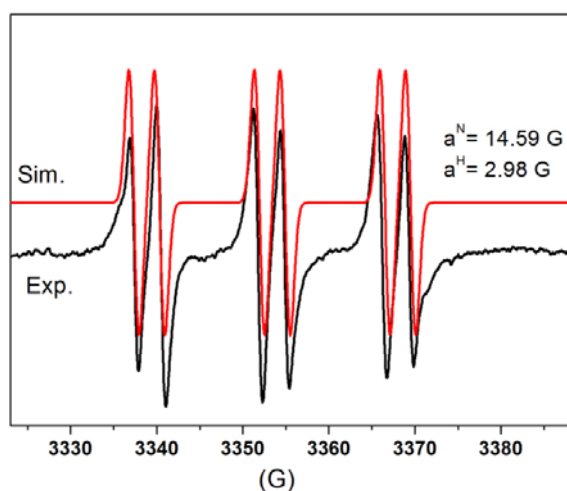
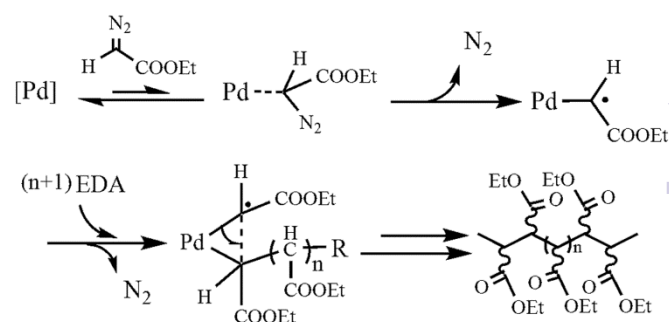


**Fig. 5** Experimental (black line) and simulated (red line) EPR spectra of poly(imidazole-Pd)-mediated polymerization of EDA at 60 °C in the presence of PBN (conditions: 30 mg poly(imidazole-Pd), 500  $\mu$ L EDA, 0.17 mmol PBN, 5 ml toluene). 2  $\mu$ L of the solution was collected and detected by room-temperature EPR.

$a^N=14.59$  G,  $a^H=2.98$  G for a PBN-trapped carbon-centred radical adduct,<sup>18</sup> indicating the existence of carbon-centred carbene radical intermediate within the reaction system.

DFT calculation on the proposed Pd-carbene radical species was also carried out to evaluate its electronic structure and spin-density distribution (BP86 density functional method with def2-SVP basis-set).<sup>34-37</sup> The calculated spin density is mainly distributed over the carbene moiety with 64.7% of spin density localized on the carbene-carbon atom and 13.9% on the carbonyl group (Fig. S8†). Conversely, the spin density on the palladium centre is low (only 14.6%). Therefore, DFT calculations on Pd-carbene radical support the EPR analyses, which assigned a significant amount of spin density on carbene-carbon atom and the Pd-carbene radical is better described as the carbon-centred Pd-carbene radical.<sup>30</sup>

Based on these results, we proposed a stepwise carbene radical migration and insertion propagation process, which is the characteristic of the newly-developed metal-carbene radical polymerization (MCRP) mechanism (Scheme 3): the pre-equilibrium binding of EDA on palladium catalyst forming the “Pd-diazo” adduct<sup>38,39</sup> is the slow initiation step; after  $N_2$  elimination forms a Pd-carbene radical, the fast migration insertion of the carbene radical into the Pd-C bond is the chain propagation process; Through the stepwise carbenoid carbon-radical migration and insertion process, polycarbene could be generated. Since most of the oligomers obtained with palladium-catalyzed system are atactic, the MCRP mechanism could well account for the formation of the atactic polycarbene. As to the stereo-selective carbene polymerization, the increased steric hindrance of the polyimidazole ligands on the palladium centre may affect the carbene radical insertion and rotation barrier, which could lead to the generation of the stereoregular polycarbene.<sup>40,41</sup>



**Scheme 3** Proposed metal-carbene radical polymerization (MCRP) mechanism.

## Conclusions

Metalloenzyme-inspired polymeric palladium catalyst was used to induce carbene polymerization, which offers high catalytic activity as well as reusability. Remarkably, besides atactic polymer, small amount of stereoregular polycarbene was also obtained with poly(imidazole-Pd)-mediated polymerization of EDA, which is the first example that stereoregular polycarbene in isolated form is obtained with a palladium-initiating system. By detailed end group analyses on the obtained atactic PCEC and stereoregular PCEC, the mechanisms of chain-initiation and termination processes were also unveiled. XPS analyses on the oxidation state changes of palladium suggest the involvement of an unusual Pd<sup>I</sup> species. Kinetic study, radical inhibition and spin-trapping experiments indicate a radical polymerization process. DFT calculations support the existence of palladium-carbene radical intermediates. We further proposed a new metal-carbene radical polymerization mechanism, which occurs through a stepwise carbene radical migration and insertion process to afford polycarbene.

## Acknowledgements

We thank for National Natural Science Foundation of China (Nos. 21274112, 21074097 and Nos. 2014203020208) for financial support. We thank Hong Yi (Wuhan University) and Jihu Su (University of Science and Technology of China) for assistance with the EPR detection and analyses. We also thank Zhi Li for language editing.

## References

1. E. Jellema, A. L. Jongerius, J. N. Reek and B. de Bruin, *Chem. Soc. Rev.*, 2010, **39**, 1706-1723.
2. A. F. Noels, *Angew. Chem. Int. Ed.*, 2007, **46**, 1208-1210.
3. E. Ihara, N. Haida, M. Iio and K. Inoue, *Macromolecules*, 2003, **36**, 36-41.
4. E. Ihara, A. Nakada, T. Itoh and K. Inoue, *Macromolecules*, 2006, **39**, 6440-6444.

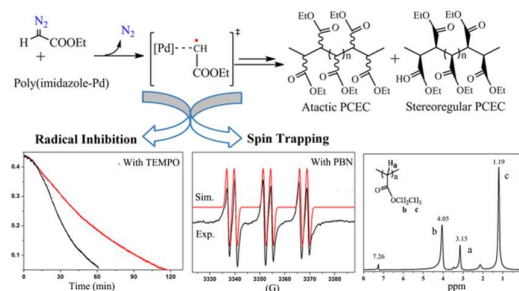


- 5 E. Ihara, Y. Ishiguro, N. Yoshida, T. Hiraren, T. Itoh and K. Inoue, *Macromolecules*, 2009, **42**, 8608-8610.
- 6 E. Jellema, P. H. M. Budzelaar, J. N. H. Reek and B. de Bruin, *J. Am. Chem. Soc.*, 2007, **129**, 11631-11641.
- 7 D. G. H. Hetterscheid, C. Hendriksen, W. I. Dzik, J. M. M. Smits, E. R. H. van Eck, A. E. Rowan, V. Busico, M. Vacatello, V. A. Castelli, A. Segre, E. Jellema, T. G. Bloembergen and B. de Bruin, *J. Am. Chem. Soc.*, 2006, **128**, 9746-9752.
- 8 A. J. C. Walters, O. Troeppner, I. Ivanovic-Burmazovic, C. Tejel, M. P. del Rio, J. N. H. Reek and B. de Bruin, *Angew. Chem. Int. Ed.*, 2012, **51**, 5157-5161.
- 9 N. M. G. Franssen, J. N. H. Reek and B. de Bruin, *Polym. Chem.*, 2011, **2**, 422-431.
- 10 L. Yang, L. Luo, S. Zhang, X. Su, J. Lan, C. Chen and J. You, *Chem. Commun.*, 2010, **46**, 3938-3940.
- 11 T. Kaliyappan and P. Kannan, *Prog. Polym. Sci.*, 2000, **25**, 343-370.
- 12 Y. M. A. Yamada, S. M. Sarkar and Y. Uozumi, *J. Am. Chem. Soc.*, 2012, **134**, 9285-9290.
- 13 Y. M. A. Yamada, S. M. Sarkar and Y. Uozumi, *J. Am. Chem. Soc.*, 2012, **134**, 3190-3198.
- 14 Y. M. A. Yamada, S. M. Sarkar and Y. Uozumi, *Angew. Chem. Int. Ed.*, 2011, **50**, 9437-9441.
- 15 L. Liu, Y. Song and H. Li, *Polym. Int.*, 2002, **51**, 1047-1049.
- 16 L. Xiao, X. Jia, L. Liao and L. Liu, *Chem. Lett.*, 2014, **25**, 1601-1606.
- 17 X. Jia, Y. Li, L. Xiao and L. Liu, *Polym. Chem.*, 2014, **5**, 4781-4789.
- 18 A. Kermagoret, A. Debuigne, C. Jerome and C. Detrembleur, *Nat. Chem.*, 2014, **6**, 179-187.
- 19 E. B. Womack and A. B. Nelson, *Org. Synth.*, 1944, **24**, 56.
- 20 A. Drelinkiewicz, A. Waksmundzka, W. Makowski, J. W. Sobczak, A. Krol and A. Zieba, *Catal. Lett.* 2004, **94**, 143-156.
- 21 J. Batista, A. Pintar, D. Mandrino, M. Jenko and V. Martin, *Appl. Catal., A*, 2001, **206**, 113-124.
- 22 A. J. C. Walters, E. Jellema, M. Finger, P. Aarnoutse, J. M. M. Smits, J. N. H. Reek and B. de Bruin, *ACS Catal.*, 2012, **2**, 246-260.
- 23 M. Finger, J. N. H. Reek and B. de Bruin, *Organometallics*, 2011, **30**, 1094-1101.
- 24 A. Gniewek, A. M. Trzeciak, J. J. Ziolkowski, L. Kepinski, J. Wrzyszc and W. Tylus, *J. Catal.*, 2005, **229**, 332-343.
- 25 O. N. Shishilov, T. A. Stromnova, J. Campora, P. Palma, M. A. Cartes and L. M. Martinez-Prieto, *Dalton Trans.*, 2009, 6626-6633.
- 26 L. Xiao, F. Li, Y. Li, X. Jia and L. Liu, *RSC Adv.*, 2014, **4**, 41848-41855.
- 27 A. Penoni, R. Wanke, S. Tollari, E. Gallo, D. Musella, F. Ragaini, F. Demartin and S. Cenini, *Eur. J. Inorg. Chem.*, 2003, 1452-1460.
- 28 D. G. Blackmond, M. S. Hodnett and G. C. Lloyd-Jones, *J. Am. Chem. Soc.*, 2006, **128**, 7450-7451.
- 29 W. I. Dzik, X. Xu, X. P. Zhang, J. N. H. Reek and B. de Bruin, *J. Am. Chem. Soc.*, 2010, **132**, 10891-10902.
- 30 H. Lu, W. I. Dzik, X. Xu, L. Wojtas, B. de Bruin and X. P. Zhang, *J. Am. Chem. Soc.*, 2011, **133**, 8518-8521.
- 31 W. I. Dzik, X. P. Zhang and B. de Bruin, *Inorg. Chem.* 2011, **50**, 9896-9903.
- 32 S. S. Shinde, M. P. Hay, A. V. Patterson, W. A. Denny and R. F. Anderson, *J. Am. Chem. Soc.*, 2009, **131**, 14220-14221.
- 33 C. L. Hawkins and M. J. Davies, *Biochim. Biophys. Acta*, 2014, **1840**, 708-721.
- 34 A. D. Becke, *Phys. Rev. A.*, 1988, **38**, 3098-3100.
- 35 J. P. Perdew, *Phys. Rev. B.*, 1986, **33**, 8822-8824.
- 36 F. Weigend, R. Ahlrichs, *Phys. Chem. Chem. Phys.* 2005, **7**, 3297-3305.
- 37 T. Lu, F. Chen, *J. Comput. Chem.* 2012, **33**, 580-592.
- 38 J. L. Maxwell, K. C. Brown, D. W. Bartley and T. Kodadek, *Science*, 1992, **256**, 1544-1547.
- 39 B. F. Straub, *J. Am. Chem. Soc.*, 2002, **124**, 14195-14201.
- 40 J. Lutz, D. Neugebauer and K. Matyjaszewski, *J. Am. Chem. Soc.*, 2003, **125**, 6983-6993.
- 41 Z. Ke, S. Abe, T. Ueno and K. Morokuma, *J. Am. Chem. Soc.*, 2012, **134**, 15418-15429.

## Polymeric Palladium-Mediated Carbene Polymerization

Feifei Li, Longqiang Xiao and Lijian Liu\*

### Table of Contents



A newly-developed metal-carbene radical polymerization mechanism is proposed for poly(imidazole-Pd)-mediated carbene polymerization, which could produce stereoregular polycarbene besides atactic polycarbene.